Article

Adaptive Mobility-Based IoT LoRa Clustering Communication Scheme

Dick Mugerwa [1], Youngju Nam [1], Hyunseok Choi [1], Yongje Shin [2] and Euisin Lee [1,*]

[1] School of Information and Communication Engineering, Chungbuk National University, Cheongju 28644, Republic of Korea; dmugerwa@kyu.ac.ug (D.M.); imnyj@cbnu.ac.kr (Y.N.); hschoi@cbnu.ac.kr (H.C.)
[2] Research Institute for Computer and Information Communication, Chungbuk National University, Cheongju 28644, Republic of Korea; yjshin@cbnu.ac.kr
[*] Correspondence: eslee@cbnu.ac.kr

Abstract: Long Range (LoRa) as a low-power wide-area technology is distinguished by its robust long-distance communications tailored for Internet of Things (IoT) networks. Because LoRa was primarily designed for stationary devices, when applied to mobile devices, they become susceptible to frequent channel attenuation. Such a condition can result in packet loss, higher energy consumption, and extended transmission times. To address these inherent challenges posed by mobility, we propose an adaptive mobility-based IoT LoRa clustering communication (AMILCC) scheme, which employs the 2D random waypoint mobility model, strategically partitions the network into optimal spreading factor (SF) regions, and incorporates an adaptive clustering approach. The AMILCC scheme is bolstered by a hybrid adaptive data rate (HADR) mechanism categorized into two approaches, namely intra-SF and inter-SF region HADRs, derived from the standard network-based ADR mechanism for stationary devices, to ensure efficient resource allocation for mobile IoT LoRa devices. Evaluation results show that, based on simulations at low mobility speeds of up to 5 m/s, AMILCC successfully maximizes the packet success ratio to the gateway (GW) by over 70%, reduces energy consumption by an average of 55.5%, and minimizes the end-to-end delay by 47.62%, outperforming stationary schemes. Consequently, AMILCC stands as a prime solution for mobile IoT LoRa networks by balancing the high packet success ratio (PSR) with reliability with energy efficiency.

Keywords: long range (LoRa); low-power wide-area network (LPWAN); Internet of Things (IoT); spreading factor (SF); adaptive data rate; mobile devices; resource allocation

1. Introduction

Recently, the Internet of Things (IoT) has garnered the attention of both industry and research communities, especially in the context of expanding IoT-centric networks [1]. The IoT offers a network of intelligent objects/sensors and devices [2], including consumer electronics. By leveraging embedded technologies to deliver and share information both among devices and with humans, enabling intelligent decision making, the IoT helps provide rapid access to information pertaining to every device while also maximizing productivity and efficiency [3]. From a conceptual viewpoint, the foundation of the IoT is built on three interrelated pillars concerning smart objects. Firstly, the capacity for self-identification (each object uniquely identifies itself). Secondly, these objects possess the ability to communicate, signifying their capacity to relay information. Lastly, the objects have the capability to interact, highlighting their ability to engage, respond, and collaborate. This interaction occurs both within their interconnected networks and with end users [4].

The IoT paradigm assigns additional capabilities to sensors and subjects them to new challenges in terms of quality of service (QoS), security [5], load balancing [6], and power control [7]. Today, a variety of data-collecting devices are already integrated into IoT platforms and applications [8] that need mobility, such as smart cities [9], smart cars [10],

and healthcare [11]. Unlike the IoT fundamentally based on static devices, the Internet of Mobile Things (IoMT) consists of mobile devices with sensors able to connect with one another as well as with surrounding cyber-physical infrastructures [12]. Cisco predicts that by 2030, 500 billion devices will be connected to the Internet [10]. It is also anticipated that by 2025, internet nodes will exist in every object, thus increasing the number of internet-connected devices and mobility control services [13]. According to the Ericsson mobility report [14], as of 2023, the number of mobile IoT devices had increased significantly, reaching 30.9 billion, with a compound annual growth rate (CAGR) of 19% observed in the preceding years.

Low-power wide-area networks (LPWANs) are a group of wireless communication technologies developed to facilitate Internet of Things deployment [2]. LPWANs represent a new paradigm in communication that bridges the gap between cellular and short-range wireless technologies to address the diversity of Internet of Things applications. These technologies are intended to provide low-power, low-cost, and low-data-rate devices with an array of functionalities, including wide-area and enormous-scale communication. This is why LPWAN technologies have aroused so much attention with the introduction of several proprietary technologies such as Long Range (LoRa) [15] and SigFox [16].

A substantial number of Internet of Things end devices are mobile, which increases the complexity of the protocols used in LPWANs. LoRa is one of the pillars of LPWAN techniques capable of long-distance message delivery and low energy consumption, making it appropriate for inexpensive devices. LoRa was originally intended for stationary devices [15]. However, it can also be used for low-speed mobile devices. In IoT LoRa networks, the Internet is pivotal in enabling connectivity between gateways and network servers, facilitating the onward flow of data to where it can be utilized effectively.

The conventional LoRa network is a low-power wireless area network that utilizes an unlicensed spectral spectrum [10]. As a result, LoRa is a cost-effective option for a variety of applications that can be adopted by anyone. Despite the fact that LoRa was not initially designed for mobile devices, numerous mobile-centric applications employ it [8]. These include tracking mobile mechanical equipment in industrial environments, collecting data via mobile sensors in smart city scenarios [9], and monitoring persons in emergency situations. Specifically, LoRa networks support single-hop communications and are primarily designed for stationary LoRa end devices (EDs) connected to a centralized gateway (GW) through a direct link. However, when this technology is adapted for mobile nodes, several challenges arise, including increased susceptibility to frequent channel attenuation. Such a condition can result in longer transmission times, massive packet loss, higher energy consumption, and interference from distant EDs with a high spreading factor [17,18]. Recent multi-hop LoRa network schemes proposed in [17,19,20] utilize explicit relay nodes and cluster-based techniques to partially mitigate the limitations of the high channel attenuation and long transmission time in the conventional single-hop LoRa by emphasizing coverage extension. However, they do not harness the mobility-based clustering technique and optimally allocate resources (e.g., spreading factor and transmit power) to static and mobile EDs simultaneously to improve connectivity with mobile LoRa nodes as well as the packet success ratio (PSR). To address the mobility of LoRa nodes, several studies have been conducted on IoT LoRa networks [21–23]. The authors of [21] investigated the usage of LoRaWAN in the field of mobile Internet of Things applications to evaluate the influence of the mobility of LoRa nodes. In [22,23], the authors proposed an enhanced adaptive data rate (ADR) mechanism based on the position of mobile LoRa nodes and a hybrid ADR mechanism based on their status (i.e., static or mobile) for allocating resources to IoT LoRa networks with mobility. However, these schemes are still susceptible to frequent channel attenuation, increased collision due to interference, frequent network reconfiguration as a result of dynamic network topology, and increased energy consumption.

To address the inherent challenges of both stationary and mobile IoT LoRa networks, we propose a structured approach based on clustering and a hybrid adaptive data rate to

manage the challenges while ensuring improved efficiency, scalability, and reliability of the network. Then, we propose an adaptive mobility-based IoT LoRa multi-hop clustering communication scheme that relies on the clustered structure within an uneven SF region environment. In our cluster structure, every cluster has a particular mobile node acting as a cluster head (CH), which gathers data from normal LoRa nodes in the cluster and delivers their fusion data to the GW on their behalf. Moreover, the proposed scheme exploits mobility patterns with a hybrid adaptive data rate (HADR) strategy that actively monitors environmental factors and automatically modifies the network resources of mobile LoRa devices (LDs) in the cluster to enhance the functionality of the network. Consequently, to achieve massive scalability and connectivity, we aim to maximize the minimum success probability of all distant LDs, the network latency, and the energy efficiency of the LoRa network.

This paper's contributions are summarized as follows:

1. We partition the network area into several distinct regions to optimize SF region allocation. Within these regions, grids maintain uniform widths, but their heights increase with the distance from the GW.
2. We devise a cohesive system model, seamlessly integrating network, success probability, energy, and mobility models, enriched further by the inclusion of the Grey relational analysis model.
3. We introduce the adaptive mobility-based IoT LoRa clustering communication (AMILCC) scheme, which comprises three main mechanisms: cluster architecture development, an efficient data forwarding mechanism, and the hybrid adaptive data rate mechanism.
4. We formulate a resource allocation strategy for mobile LoRa devices in the AMILCC scheme using a hybrid adaptive data rate (HADR) mechanism. This mechanism is categorized into two approaches: (1) intra-SF region HADR, and (2) inter-SF region HADR.
5. We conduct simulations in various environments to evaluate the performance of the proposed AMILCC scheme at varying speeds. By comparing it with existing stationary schemes, the excellence of the AMILCC scheme is verified through performance evaluation metrics such as the packet success ratio, energy consumption, and end-to-end delay.

The rest of this paper is organized as follows. In Section 2, we elaborate on the related works on IoT LoRa techniques. Section 3 provides the system model for the proposed AMILCC scheme, which includes a network model, a success probability model, an energy model, a mobility model, and a Grey relational analysis model. In Section 4, we describe the proposed AMILCC scheme in detail. The performance evaluation of the proposed AMILCC scheme is presented through simulation results in Section 5, which are then discussed in Section 6. Finally, this paper concludes in Section 6.

2. Related Works

LoRa is a leading LPWAN technology developed by Semtech, known for its long-distance and low-power communication capabilities using a proprietary Chirp Spread Spectrum modulation. This technology operates on license-free ISM bands below 1 GHz and enhances phase continuity between chirps in a packet's preamble, simplifying timing and frequency synchronization without costly components for stable clock generation. LoRa's performance, as discussed in [24,25], hinges on the link budget—adjustable through the code rate (CR), bandwidth (BW), transmission power (Tx), and spreading factor (SF). With BW options from 7.8 kHz to 500 kHz, wider BWs facilitate higher data rates and reduced airtime. LoRa employs Forward Error Correction (FEC) to mitigate interference, with the CR influencing transmission reliability versus airtime. The spreading factor, $SF \in \{7, \dots, 12\}$, defines the chirp symbol length [26]. LoRaWAN, the MAC layer defined by the LoRa Alliance, operates primarily on an ALOHA protocol, as per [15], with the adaptive data rate (ADR) optimizing the balance between energy use and network resilience by adjusting the SF. LoRaWAN delineates three device classes: Class A (all), Class B (beacon), and Class C (continuous listening), each tailored to specific operational modes.

2.1. Multi-Hop Communication between LoRa Devices

Multi-hop communications are utilized to increase the connection's range beyond that of single-hop communications. Numerous studies have been published on IoT LoRa networks to enable the coverage extension of single-hop communications-based IoT LoRa networks. LoRablink [27] is one of the earliest LoRa-based multi-hop networks. It utilizes an IoT TDMA protocol designed to allow energy-efficient and dependable multi-hop communication. In [17], the authors suggested a selective relay-based multi-hop communication method known as fair and scalable relay control (FSRC). The relay control technique employed by FSRC maximizes both the coverage probability and minimum success probability across all SF regions by regulating communication parameters. As with other comparable schemes [20,28], the authors introduced a programmed e-node and an implicit relay node to function as a transparent range extender with an overhearing operation, respectively. With the primary objective of replicating the identical packet delivered by the remote end devices, they overhear the transmission and relay it to the GW. However, both methods generate a substantial amount of network traffic due to broadcasts, which degrades performance.

2.2. Clustering of Mobile IoT LoRa Devices

In clustering for IoT LoRa networks, LoRa devices are grouped into specific SF clusters, and the CH in each cluster mediates data flows between LoRa devices and the GW. Clustering enhances network connectivity and extends the lifespan of wireless networks by efficiently managing nodes [19]. It minimizes packet duplication, optimizes data routing, and improves efficiency and scalability while eliminating redundant message delivery. Consequently, various cluster-based approaches have been proposed for IoT LoRa networks, underscoring the importance of clustering as a key mechanism for facilitating efficient communication among LoRa nodes. In [29], a strategy combining a forwarding relay node with clustering enhanced LoRa network coverage and energy efficiency through multi-hop communication, although it increased traffic and redundancy. Ref. [19] introduced an SF-based clustering scheme to boost multi-hop capacity, assigning unique SFs to clusters around sink nodes, but it faced challenges in network maintenance due to the impractical removal of devices from higher SF clusters. Meanwhile, Ref. [30] proposed an SF partition-based clustering and relaying (SFPCR) scheme aimed at improving packet delivery success across SF regions, yet it failed to account for the mobility of IoT LoRa devices, limiting its effectiveness in dynamic settings.

2.3. Mobility for IoT LoRa Networks

Mobility in sensor networks enables nodes to move after their initial placement, as highlighted in the existing literature, which categorizes mobility into mobile nodes and mobile sinks [31]. This capability is crucial for improving network performance through hotspot resolution, topology optimization, congestion reduction, and energy savings. LoRa, typically used in static settings, also finds relevance in mobile scenarios such as fleet monitoring, bike rentals [32], and wildlife tracking, indicating the need for exploring mobility models in LoRa networks [21]. The authors of [33] explored a QoS-aware adaptive mobility method in LoRa-based IoT, focusing on the impact of mobile node configurations on network reliability and efficiency.

The use of mobile IoT technologies, such as e-scooter services in Korea [34], exemplifies the potential for environmental data collection within LoRa networks, including monitoring variables like temperature and humidity. Studies like those in [22,35] emphasize the importance of mobility in the IoT, with the latter enhancing LoRaWAN's ADR mechanism for better prediction of mobile device positions. Surveillance systems integrating LoRa and BLE for varied applications were discussed in [36,37]. Meanwhile, research into LoRa's mobility, particularly with UAVs, has identified diverse mobility models without settling on an optimal pattern for specific IoT services, highlighting a need for standardized performance assessment methods [38,39].

3. System Model

In this section, we provide a detailed description of the system model in the proposed AMILCC scheme. We first present the network model, success probability model, energy model, and mobility model. Next, we derive the Grey relational analysis model.

3.1. Network Model

The geographical area covered by one GW is partitioned into uneven SF regions depending on the distance from the GW, as shown in Figure 1. These partitions also represent clusters of LDs/CMs with a single CH communicating with the GW. This ensures that only a few LDs communicate with the GW, thereby avoiding network congestion, packet collisions and losses, delayed packet transmission and acknowledgment, etc. Each LD in a particular partition or cluster only communicates with its CH. The partition closest to the GW has a lower SF value, and its CH can communicate with a higher DR with the GW. The farthest partition h_n has the highest SF of 12, and the CH here must use the lowest DR to ensure reliable communication with the GW. The width (W) of each partition is fixed. However, the height (h) of each partition increases at a fixed ratio of 1.5. Both the W and h are measured in meters. The LDs are randomly distributed across the network, as shown in Figure 1, with each partition containing a random number of LDs. The basic assumptions are as follows:

- The LDs are mobile and can change their partitions.
- The CHs are mobile, whereas the GW remains stationary.
- The LDs follow a set predetermined path and network topology can be altered.
- All LDs possess omni-directional antennas.
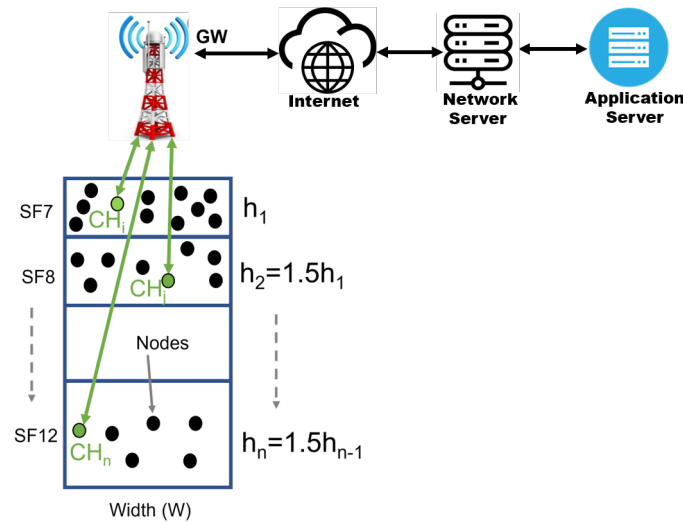- Any two LDs cannot be at the same (X, Y) position in the given 2D coverage area.

Figure 1. Model of the SF region partition process in the proposed AMILCC scheme.

The GW will broadcast a network initialization message in the form of beacons when the network deployment is complete. The GW will determine the LDs' positions and SFs based on the strength of the received broadcast signal [40]. An uplink is the data frame transmitted from an LD to the GW, and a downlink is defined as the data frame transmitted from the GW to an LD. The notations used in this article are summarized in Table 1.

We form clusters of mobile IoT LoRa devices in different SF regions with a finite number of cluster heads (CH > 1). The collection of all CHs is CH ={CH1, CH2, ... CHn}, where n is the partition or cluster number, and each CH has a coordinate (X_i, Y_i). We assume that sensor environment A contains mobile nodes with LD > 0, denoted by $LD = \{Ld_1, Ld_2, \ldots, Ld_m\}$, and that mobile nodes move along a predetermined path via vision. The topology of the network can be altered, and the LoRa nodes can move with a minimum speed of 0.5 m/s and a maximum speed of 5 m/s. Let $P = \{p_1, p_2, \ldots, p_m\}$ and velocity

$V = \{v_1, v_2, \ldots, v_m\}$ represent the sets of paths and velocities, respectively. According to [1], mobility in LoRaWAN can only be achieved in the uplink. When an end node moves, its location changes, and at the same time, it can send data. This can be achieved using any of the three classes without latency as long as it is within the coverage of LoRaWAN network GWs. Figure 2 illustrates the trajectory of an IoT LoRa mobile device LD(i), following the random waypoint (RWP) model over time *t*, emphasizing the mobility pattern of the node. Here, we obtain the mobile node's moving distance $d_i = v_i \times t$ during a given period, and the coordinates of LD(i) change from (X_0, Y_0) to (X_1, Y_1). The communication trajectory sequence (T_i) of LoRa mobile device LD(i) along a path (p_i) contains a series of moving positions over a given period t, $T_i = \{(x_0, y_0), (x_1, y_1), \ldots (x_n, y_n)\}$.

Table 1. List of main notations.

| Symbol	Description
T_i	Trajectory sequence
$P_{success}^i(location(x))$	Probability of successful transmission
$T_{SF(i)}$	Time on air
$I_{SF(i)}$	Number of potential interferences
R_b	Data rate
SF(i)	Spreading factor of a LoRa device
$E_{tx,i}$	Transmission time
$E_{n-Hops}(SF, P_{tx(i)})$	Energy consumption of *n* hops
$E_{tot\_i}(t)$	Total energy consumption
$Ec_s(i)$	Energy consumption of a LoRa device
$E_{re\_i}(t)$	Residual energy of a node at time (*t*)
$RS(i, j, t)$	Relative speed
$d(m_i, m_j)$	Euclidean distance
$X_{ij(norm)}$	Normalized values
S_{ij}	Grey relational coefficient
Δ_{ij}	Absolute difference between values
G_i	Grey relational grade
NR_{new}	Network resource
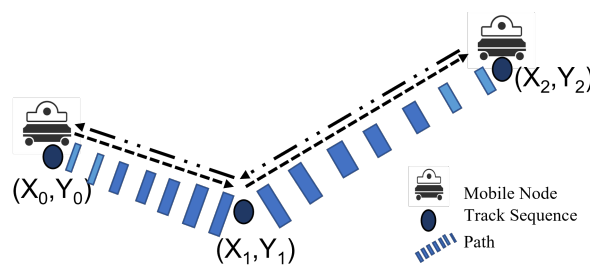
Figure 2. IoT LoRa mobile node movement path.

The performance of LoRaWAN is influenced by the duty cycle limitation in the 868 MHz band, restricting the time on air (ToA) for packet transmission to a duty cycle (δ_i) of 1%, with a code rate (CR) of 4/5 and a bandwidth (BW) that varies between 125 kHz and 500 kHz. We focus on deploying Class B LoRa devices that initiate transmission, transmitting packets during their slot time without interference using spreading factors (SF) ranging from 7 to 12. An initial SF allocation (I-SFA) scheme [41] was utilized to adaptively assign SFs to LoRa devices (LDs) at deployment, based on the signal strength received at the gateway (GW) and accommodating variable channel conditions such as shadowing and fading. The network employs a star topology for direct communication between end nodes and GWs, where scheduling beacon messages transmitted by moving LoRa nodes, containing information like node ID, status, and time interval, becomes crucial due to the volume of messages.

3.2. Success Probability Model

To ensure reliable communication between LDs and CHs/GW, an important factor is the link quality (LQ) in a particular SF partition. The LQ model given in [30] is used to enable frame transmission without collision and with all frame bits correctly decoded despite the presence of interference. However, due to harsh environmental and unavoidable data capture effects, not all bits transmitted to the GW by LDs can be received. Therefore, a reliable transmission LQ is an essential parameter for an acceptable packet delivery ratio in multi-hop communication to the GW. Let us assume that a particular LD starts transmitting, no other LD transmits for a critical time duration given by $2T_{SF(i)}$, and the probability of successful transmission by an LD at location x in a particular partition is given by $P^i_{success}(location(x))$ in Equation (1),

$$P^i_{success}(location(x)) := e^{-2T_{SF(i)}\varphi I_{SF(i)}} \tag{1}$$

where $T_{SF(i)}$ is the time on air, $I_{SF(i)}$ is the number of potential interferences within the same spreading factor region, and φ is the packet transmission intensity.

3.3. Energy Model

In the AMILCC scheme, we utilize the energy model from [28] for continuity and direct comparison of performance metrics under various conditions of LoRa devices, which differ from Class C devices that rely on mains power. The energy consumption, $E_{tx,i}$, for a LoRa device (LD(i)) sending a β-bit packet includes the stages of activation, low-power listening, radio setup, transmission, deactivation, and processing. Moreover, the energy for transmission is influenced by both the power and SF-dependent transmission duration, as defined in (2) [42],

$$E_{tx,i} = P_{tx(i)} \times T_{SF(i)} \tag{2}$$

where P_{tx} is the transmission power with the ToA for LD(i) with $SF(i)$, and $T_{SF(i)}$ denotes the time on air for LD(i).

The energy consumption for sending a packet using multi-hop communication with n hops between LD(i) and GW is given by $E_{n-Hops}(SF, P_{tx(i)})$, as shown in Equation (3).

$$E_{n-Hops}(SF, P_{tx(i)}) = \sum_{i=1}^{n}(E_{tx,i} + E_{rx,i}) \tag{3}$$

Here, $P_{tx(i)}$ is the transmission power, and $E_{tx,i}$ and $E_{rx,i}$ are the energy consumption of the transmitter and receiver, respectively, for the i-th hop according to the current setting for $P_{tx(i)}$, SF, and BW.

Most LDs are usually of Class A or B, so they mostly remain in sleep mode to ensure lower energy consumption and preserve battery life. Thus, for the total energy consumption of an LD(i) at time t, $E_{tot\_i}(t)$, given by Equation (5), we consider two states, inactive or sleep mode ($E_{sle\_i}(t)$) and active mode ($E_{act\_i}(t)$), given by Equation (4), which is made up of the energy consumption during transmission, reception, processing, and wake up. This dynamic switching from sleep mode to active mode in LoRa devices impacts the power consumption of LoRa devices, and the frequency and duration of these transitions can significantly affect the device's battery life.

$$E_{act\_i}(t) = E_{Wp} + E_{proc} + E_{Wut} + \sum_{j=1}^{n} Ec_s(i) \tag{4}$$

$$E_{tot\_i}(t) = E_{sle\_i}(t) + E_{act\_i}(t) \tag{5}$$

$E_{sle\_i}(t)$ represents the dissipated energies in the state when devices are in sleep mode ($E_{sle\_i}(t)$). In active mode ($E_{act\_i}(t)$), E_{Wp} represents the energy consumption when a device wakes up, E_{proc} represents the energy consumption of data processing, and E_{Wut} represents

the amount of energy to move the transceiver from sleep mode to active mode. In addition, $Ec_s(i)$, as calculated in Equation (6), represents the energy consumption of LD(i) for a particular DR to transmit X_{packet} with *n* hops.

$$Ec_s(i) = \frac{X_{packet}}{R_b} \times (P_{tx}(i) + P_{rx}(i)) \tag{6}$$

$$R_b = \frac{CR \times SF}{\frac{2^{SF}}{BW}} \tag{7}$$

Here, X_{packet} is the size of the transmitted packet in bits; $P_{tx}(i)$ and $P_{rx}(i)$ are the consumed power according to the supply current and supply voltage for the transmitter and receiver, respectively; and R_b is the bit rate defined in Equation (7). *CR* is the code rate defined as $\frac{4}{(\iota+4)}$ with $\iota \in \{1, 2, 3, 4\}$. Ultimately, to understand an LD's energy consumption, it is essential to efficiently utilize the LD's residual energy $E_{re\_i}(t)$ at a given time (t) for the effective selection of CHs and also to prevent the untimely demise of devices to ensure that the energy of each LD in the network is consumed in a relatively balanced manner. Thus, $E_{re\_i}(t)$ can be computed as (8),

$$E_{re\_i}(t) = E_0 - E_{tot\_i}(t) \tag{8}$$

where E_0 is the initial energy of LoRa devices.

3.4. Mobility Model

A reliable LoRa mobility model is required for efficient positioning and range determination of LDs in the coverage zone of each GW. Despite the fact that LoRaWAN was designed for static low-power long-range networks, several IoT solution applications involve the use of mobility [21]. Therefore, we consider a dynamic mobility pattern where the movement is based on the medium that the node moves through. A dynamic 1D, 2D, or 3D mobility path is assumed for each LD, whose movement depends on the medium through which it moves. In the proposed AMILCC scheme, which is optimized for low mobility, we employ the random waypoint (RWP) model from [43]. In the RWP model, each LD follows a continuous sequence of pauses and motions. During the pause duration of 0 to 20 s, the LD maintains its latest position, and during the motion period, it starts moving at a random speed varying from 0 to 5 m/s in a random direction until it pauses again in a network consisting of one GW. If the coverage boundary is reached, the direction of the LD is reversed, and the pause-motion sequence continues. There must be some mobility measuring metrics for LDs like those given in [44]. Also, the relative speed (RS) metric can be used to differentiate the movement patterns of LDs using their relative motion or speed. We assume that LD(i) and LD(j) move with speeds $\vec{V}_i(t)$ and $\vec{V}_j(t)$, respectively. Their RS is computed using Equation (9). It should be noted that the RS can impact network and node clustering performance. The RS can effectively serve as one of the key parameters in adaptive clustering algorithms for clustering LDs. For example, LDs with similar speeds can lie in the same cluster, while nodes moving at different speeds can be placed in different clusters.

$$RS(i, j, t) = |\vec{V}_i(t) - \vec{V}_j(t)| \tag{9}$$

3.5. Grey Relational Analysis (GRA) Model

In previous sections, different models were described for determining the metrics that affect LoRa network performance, like link quality (LQ), mobility, and residual energy. The GRA model [45] is a multi-criteria technique that consolidates the three metrics into a unified metric. It has four main processing stages: (1) normalization of input data, (2) Grey relational (reference) sequence generation, (3) Grey relational coefficient computation, and (4) Grey relational grading (ranking of coefficients for decision making).

4. Adaptive Mobility-Based IoT LoRa Clustering Communication Scheme (AMILCC)

In this section, we explain the proposed adaptive mobility-based IoT LoRa clustering communication scheme in detail, which has three main mechanisms. First, we provide a detailed explanation of the cluster architecture development, followed by the data forwarding mechanism, and conclude with the hybrid adaptive data rate mechanism.

4.1. Cluster Architecture Development Mechanism

This subsection expounds on the procedure for the local cluster formation, followed by the CH selection process. Concisely, the clustering scheme generates balanced and stable clusters within the coverage region of a GW and readily updates the clusters when low-speed LDs move from higher to lower SF regions (nearer to the GW). It allows for clusters whose structure adapts to changing network conditions, positions, and paths of moving LDs.

4.1.1. Cluster Formation

The cluster formation scheme is based on adaptive DBSCAN used in [46], a density-based clustering technique that is ideal for grouping nodes based on their geographical distribution with varying densities and shapes. This can be beneficial for locating regions with a high concentration of mobile nodes and following their movement patterns over time. Figure 3 illustrates the AMILCC scheme for mobile IoT LoRa devices, combining cluster formation and communication into a cohesive framework. Figure 3a depicts how mobile LoRa devices (LDs) form density-based clusters within a defined radius r_0, achieving a minimum neighborhood device count (LD_{min}) through k-nearest neighbors analysis. Figure 3b illustrates the internal cluster connectivity, showing how cluster members connect with CHs, which, in turn, facilitate communication with the gateway (GW). This streamlined depiction not only simplifies the understanding of the clustering mechanism but also highlights the pivotal role of CHs in ensuring effective data transmission and network efficiency. Given that k is equivalent to LD_{min}, a value of 4 was selected for k. Consequently, the distance to the four nearest neighbors from any given LoRa device is calculated as the Euclidean distance between LD(i) and its four nearest neighbors. To determine the radius r_0, the Euclidean distance $d(m_i, m_j)$ between any k mobile neighbors is computed using Equation (10), where m_i is a core LD and m_j is any other LD in the neighborhood. The parameter k is determined using Equation (11), and radius r_0 is given by Equation (12), where $m_j \in J_i$, and J_i contains m_i's k nearest neighbors.

$$d(m_i, m_j) = \sqrt{(X_{m_i} - X_{m_j})^2 + (Y_{m_i} - Y_{m_j})^2} \tag{10}$$

$$k = min(LD_{max}, LD_{min}) \tag{11}$$

where LD_{max} is the maximum number of neighbors within a random cluster distance d_{max} and LD_{min} is the minimum number of mobile LDs required to make a local sub-cluster.

$$r_0 = \underset{i}{argmax}\,(d(m_i, m_j)) \tag{12}$$

If the number of LDs in the neighborhood of a reference LD is $\geq LD_{min}$, a new cluster will be created and the clusters expanded using the two important concepts of density-reachable and density-connected.
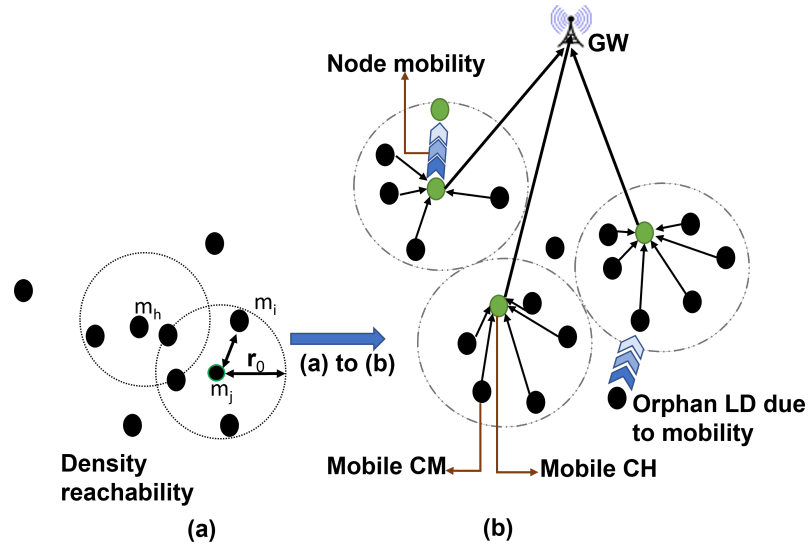
Figure 3. Adaptive mobility clustering for mobile IoT LoRa devices.

4.1.2. Cluster Head Election

After any LD cluster is formed, the cluster head (CH) is selected using the GRA consolidated metric comprised of the link quality ($P_{succuss}^{i}(location(x))$), residual energy ($E_{re\_i}(t)$), and mobility ($RS(i, j, t)$) of all mobile LDs within the local cluster, through the following steps:

- Define the objective function (X) for selecting the CH. It is comprised of multiple criteria defined by X_1, X_2, and X_3 represented by Equations (1), (8), and (9), respectively.
- Normalize the data fed to each criterion to make it comparable by dividing it by the range of data values, where the normalized value of the criterion $X_{ij(norm)}$ for LD(i) and the j-th criterion are given by Equation (14). X_{ij} is the original value of criterion j for LD(i), and $min(X_{ij})$ and $max(X_{ij})$ are the minimum and maximum values, respectively. The reference target for all criteria is X_{0j}, in which all the performance values are 1.

$$X_{ij(norm)} = \frac{(X_{ij} - min(X_{ij}))}{(max(X_{ij}) - min(X_{ij}))} \tag{13}$$

- Determine the Grey relational coefficient given by S_{ij} in Equation (14) that represents the closeness of the normalized value $X_{ij(norm)}$ to the reference X_{0j}. Δ_{min}, Δ_{max}, and Δ_{ij} are defined in Equations (15)–(17), respectively. Value Δ_{ij} is the absolute difference between X_{0j} and $X_{ij(norm)}$ and represents the deviation from the target value or quality loss. The value Δ_{min} is the lowest, and Δ_{max} is the highest value among the quality loss parameters. The parameter ρ is a coefficient within the range $0 \leq \rho \leq 1$ that can be altered if required by the system.

$$S_{ij} = \frac{\Delta_{min} + \rho\Delta_{max}}{\Delta_{ij} + \rho\Delta_{max}} \tag{14}$$

$$\Delta_{ij} = \left| X_{0j} - X_{ij(norm)} \right| \tag{15}$$

$$\Delta_{min} = min\{\Delta_{ij}, i = 1, 2, \ldots, m, j = 1, 2, 3\} \tag{16}$$

$$\Delta_{max} = max\{\Delta_{ij}, i = 1, 2, \ldots, m, j = 1, 2, 3\} \tag{17}$$

- Determine the Grey relational grade G_i for LD(i) using Equation (18). The value n is the number of nodes in a cluster, and S_{ij} is the Grey relational coefficient for LD(i). The CH of the cluster is the node with the highest G_i. The clusters are reconfigured every 10 min to adapt to node positions and changes in network topology. This

is accomplished by sending broadcast messages to all nodes in the network with information about where and when the GW will be available.

$$G_i = \frac{\left(\sum_{j=1}^{n} S_{ij}\right)}{n}, i = 1, 2...., n \qquad (18)$$

Our proposed AMILCC scheme is designed to dynamically adapt by selecting alternative cluster heads (CHs) as needed based on a set of criteria, including the residual energy levels of current CHs. When a CH's residual energy falls below a predefined threshold, the GW automatically initiates a process to nominate a replacement CH from the candidate set of available nodes. This approach ensures that no single node is overburdened with the CH role, thereby preserving the overall energy efficiency and longevity of the network. By carefully scheduling active and sleep modes and possibly rotating the CH role among multiple mobile LoRa devices, this dynamic switching from sleep mode to active mode in LoRa devices impacts power consumption. When a LoRa device transitions from sleep mode to active mode, it requires additional energy to power up its components and perform the required tasks, such as receiving and transmitting data. This increase in power consumption during the transit period contributes to the overall energy usage of the devices.

4.2. Data Forwarding Mechanism

During this phase, data are sent from the LoRa devices (LDs) to the cluster heads (CHs) and then to the gateway (GW). To achieve this, the LDs collect data and then send it to their respective CHs following scheduled time slots. The CH aggregates and compresses the data from all LDs in its cluster, and the CH also forwards the data to the GW. Each CH maintains a list of the connected LDs. Before entering their time slot, each LD rouses itself and returns to its sleep state according to the Time-Division Multiple Access (TDMA) schedule. Next, each mobile LoRa device modifies its SF and Tx adaptively to send data according to the distance between itself and the CH, which can be determined from the node information in the received data packet. Finally, the CH must remain in the "ON" state in order to receive data and sustain a connection between the CH and the GW.

After not hearing from a node for two consecutive frames, the node is deemed to have moved outside the cluster range and is consequently deleted from the list. The CH updates and distributes the TDMA schedule to related LDs. If the LD does not receive an acknowledgment (ACK) from the CH, it perceives itself to be an orphan due to its mobility. The orphaned LD can solicit a new CH and associate with it by issuing a join request (Join-Req). When a new LD joins a CH, the CH updates its node list. The CH adjusts its TDMA schedule and communicates it to all nodes within the cluster. In the proposed AMILCC scheme, each cluster member spontaneously transmits data to the CH in accordance with the TDMA schedule, and the CH aggregates the data and transmits it to the GW in multi-hop mode. As a result, once the packets are received, the CH returns the acknowledgments to the cluster members. When cluster members receive the acknowledgment signal from the CH, it means that the packets were successfully transmitted.

4.3. Hybrid Adaptive Data Rate (HADR) Mechanism

In this section, the resource allocation approaches aimed at ensuring the regular maintenance and optimization of IoT LoRa network resources for the efficient and reliable operation of mobile clusters are examined. Maintaining the stability of clusters and the network integrity of wireless networks with mobile nodes is an essential feature since mobile nodes can enter and exit clusters, generating instability and impacting network performance. A node undergoes a topological change when it disconnects and reconnects with all or some of its neighbors, thereby altering the cluster's structure.

We develop a mechanism based on the HADR [23] to maintain clusters of mobile LD-based networks by combining the static and dynamic DRs of the LDs based on the signal-to-noise ratio (SNR) of the received packets. Our scheme not only operates as a

low-pass filter to resist rapid changes in the SNR of received packets at the network server but also aims to allocate the optimal spreading factor (SF = 7~12) and transmit power (Tx = 2~14 [dBm]) to both static and mobile LDs by seeking to reduce the convergence periods. In our proposed AMILCC scheme, we have further refined the categorization of the hybrid ADR mechanism, classifying it into two distinct approaches: (1) intra-SF region HADR, and (2) inter-SF region HADR.

4.3.1. Intra-SF Region HADR

This approach enables the efficient use of network resources by dynamically varying the DR to match the quality of the communication link within a particular SF region. When employing it on mobile LDs in clusters, each LD changes its DR, Tx, and SF based on the received signal quality of its transmissions computed by the network server (NS). The scenario where an LD moves in the same SF region from its initial location (x_1, y_1) to (x_2, y_2) is considered. This scenario has a negligible effect on the SF because the received signal strength at the GW may exhibit minimal variation. If the SNR is high, indicating good link quality (LQ), the mobile LD can raise its SF to extend its range and improve its interference resistance. In contrast, if the SNR is low, the LD can reduce its SF to increase the data throughput and shorten the transmission time, as concisely shown in Algorithm 1. In this case, we envisage the settings of LD(s) with the received signal strength not exceeding a given threshold [47].

Algorithm 1: Adaptive SF selection

Input: $SNR(LD_i)$: SNR for a LoRa device
Input: SNR_{LD_i}: Current Signal-to-Noise Ratio
Input: SF_i: Current Spreading Factor
Output: SF_{New}: Adjusted SF

1: **for** $i \leftarrow 0$ to N **do**
2:     Set predefined thresholds for SNR
3:     **if** $SNR_i > SNR_{MAX_{threshold}}$ **then**
4:         $SF_{New} = SF_i + SF_{Increment}$
5:     **else if** $SNR_i < SNR_{MIN_{threshold}}$ **then**
6:         $SF_{New} = SF_i - SF_{Decrement}$
7:     **else**
8:         $SF_{New} = SF_i$
9:     **end if**
10: **end for**
11: `return` SF_{New}

4.3.2. Inter-SF Region HADR

This approach allows a mobile LD to adapt its transmission settings to the current medium's condition as it traverses several SF regions. In particular, a mobile device LD(i) moves from location (x_1, y_1) to locations (x_2, y_2) and (x_n, y_n) around the GW at times t_0 and t_n, respectively. The network server regularly monitors the SNR and the packet loss ratio (PLR) of the received packets and utilizes this information to decide the ideal SF, BW, DR, and Tx for the LD's subsequent transmission, thereby ensuring reliable communication while conserving battery power. The LD adapts its DR, SF, Tx, and BW based on the PLR and SNR thresholds. If both the PLR and SNR are below the threshold, the DR is increased. If the maximum DR has been reached, the LD decreases the BW, and if the BW is already at its minimum point, the device increases its Tx. If the maximum Tx has been reached, the LD decreases its SF. If the PLR is above the threshold or the SNR is below the threshold, the LD decreases its DR, BW, Tx, or SF, depending on which parameter is already at its lowest. As the LDs move across different SF regions, the network resources are constantly adjusted to ensure reliable communication with the GW or the nearest CH, as shown in Algorithm 2.

Algorithm 2: Inter-SF network resource adaptation

Input: *Inc*: Increase
Input: *Dec*: Decrease
Input: PLR_i: Current Packet Loss Ratio
Input: SNR_i: Current Signal-to-Noise Ratio
Input: Tx: Current Transmit power
Input: DR, BW: Current Data Rate, Bandwidth
Input: NR_{new}: New Network Resources

1:   $NR_{new} = Null$
2:   **for** $i \leftarrow 0$ to N **do**
3:       Set predefined threshold (Th) for PLR and SNR
4:       **if** $(PLR_i < PLR_{Th}) AND (SNR_i > SNR_{Th})$ **then**
5:         $i \leftarrow Inc(DR, Tx)$: unless at max
6:         $i \leftarrow Dec(BW, SF)$: unless at min
7:       **else**
8:         $i \leftarrow Dec(DR, Tx)$: unless at min
9:         $i \leftarrow Inc(BW, SF)$: unless at max
10:     **end if**
11:     $NR_{new} \leftarrow i$
12:   **end for**
13:   return NR_{new}

---

5. Performance Evaluation

In this section, we first describe our simulation environment, model, and performance evaluation metrics. Then, we compare the performance of the proposed scheme with various low mobility speeds. Finally, we evaluate the performance of the proposed AMILCC scheme in comparison with previous static communication schemes through simulation results.

5.1. Simulation Environment

We consider Class A LoRa devices (N) in a geographical region covered by a single GW and subdivide them into distinct SF regions based on distance from the GW within a 6000 m × 1000 m area. The LDs are distributed at random throughout the network, with each partition containing an arbitrary number of LDs. These LDs adhere to the European region's frequency regulation, which limits the uplink (UL) duty cycle of LDs and GWs to 1% and 10%, respectively, for the default channels. The mobility of LDs follows a two-dimensional (2D) random waypoint mobility model. LDs choose a speed varying between 0 and 2 m/s at random and shift direction every 1000 m [48,49]. During the simulation, each LD transmits an uplink packet every 600 s with varying payload sizes for 24 h of simulation time. While the lower-frequency operation of LoRa aids in better penetration through obstacles, we recognize that physical barriers can still influence signal propagation. In practice, the purpose of this paper is not to focus on efficiently dealing with obstacles. Nevertheless, to comprehensively address this issue, our methodology integrates adjustments in simulation models to incorporate obstacle dynamics and the utilization of the hybrid adaptive data rate (ADR) mechanism for optimal communication settings amidst varying environmental factors. Significantly, we incorporate the random waypoint (RWP) model into our simulations to realistically represent the mobility patterns of devices. This is supplemented by strategies like multi-hop communication for enhanced connectivity in obstructed areas and strategic network planning for effective device placement. Together, these approaches form a robust framework for assessing and mitigating the impact of obstacles on mobile LoRa networks in our research. Subsequently, we use the Free-Space Path Loss (FSPL) model, which typically uses a value of around 2 as the Path Loss Exponent (PLE) because it accurately reflects the propagation characteristics of electromagnetic waves

in free space. The FSPL model with a PLE of 2 is often appropriate for line-of-sight (LOS) communication environments where there are minimal obstructions or reflections that could attenuate the signal. In contrast to the performance of the stationary model, we modeled multi-hop communication in LoRa networks with an adaptive clustering method of LDs to extend packets to the GW using MATLAB R2023b and Simulink. This simulator was selected due to its extensive support for a variety of IoT protocols and wireless networking capabilities. As part of the initial deployment, each node's SF is set to $(SFset) = (SF_{min}, \ldots, 12)$, where SF_{min} is the minimum permissible SF for its respective SF area. During the initial setup phase, this is referred to as an(I-SFA. This method helps to limit the possible SF options at each LD, thereby reducing the learning time. Table 2 shows all the simulation parameters adopted in the simulation environment.

The metrics used for the performance evaluation of the proposed AMILCC scheme and the existing stationary model include the probability of successful transmission and the number of packets. More specifically, the metrics are as follows:

- Packet Success Ratio (PSR): This is calculated as the ratio of the total number of data packets successfully received by the network server to the total number of data packets generated by all LDs throughout the simulation period. The PSR solely defines the data packets and does not reflect the success ratio of the join request.
- Energy Consumption: This is the average amount of energy consumed by each individual LD throughout the simulation period. It is calculated as the ratio of the total amount of energy consumed by the whole network to the number of participating LDs in the network.
- End-to-End Delay: This is defined as the total time taken by a single packet to be delivered to the final destination over a LoRa-based network. The end-to-end delay can vary depending on several factors, including signal quality, SF, distance between the LD and the GW or any other receiver, interference, and environmental conditions.

Table 2. Simulation parameters.

Parameter	Values
GW	1
Network size	6000 m $\times$ 1000 m
Number of nodes (N)	1000
Mobility model	RWP
Minimum speed	0.5 m/s [48]
Maximum speed	5 m/s
Channel frequency	868 (MHz)
Spreading factor (SF)	7–12
Bandwidth	125,250,500 (kHz)
Payload length	30 (Bytes)
Transmission power	2–14 dBm (25 mW)
Data rate	0.25–5.47 (kbps)
Coding rate	4/5
Simulation time	24 hrs
Payload CRC	ON
Interval time	600 s
Path loss exponent	2

5.2. Simulation Results

In this section, we first evaluate various speeds to ascertain the most suitable speed for the mobile LDs in the proposed AMILCC scheme. Then, we examine the effects of various low mobility speeds (1, 2, and 5 m/s) on network performance, specifically assessing the PSR and end-to-end delay. Subsequently, we present the obtained results of the performance evaluation metrics using both mobile and static LD communication transmission parameters.

Figure 4a shows the PSR as a function of the number of devices and mobility speed. The results show that node mobility has an ameliorated impact on the PSR of the proposed AMILCC scheme using the random waypoint mobility model, which contrasts with the results in [21]. At movement speeds of 2 m/s or below, the AMILCC scheme can conveniently cluster mobile LDs to yield good performance, where more than 70% of data packets are successfully delivered to the GW. This good performance is also maintained with an increased number of nodes in the network. However, as the movement speed of the LDs increases up to 5 m/s, we observe that the PSR of the transmitted packets gradually deteriorates. This occurs because of path-breaking due to the faster movement of the LDs. Without loss of generality, it should be noted that this good performance in terms of the PSR of slower mobile nodes is attributed to a stable connection, fewer threshold-based handovers from one CH to another, and less frequent location updates of mobile LDs.
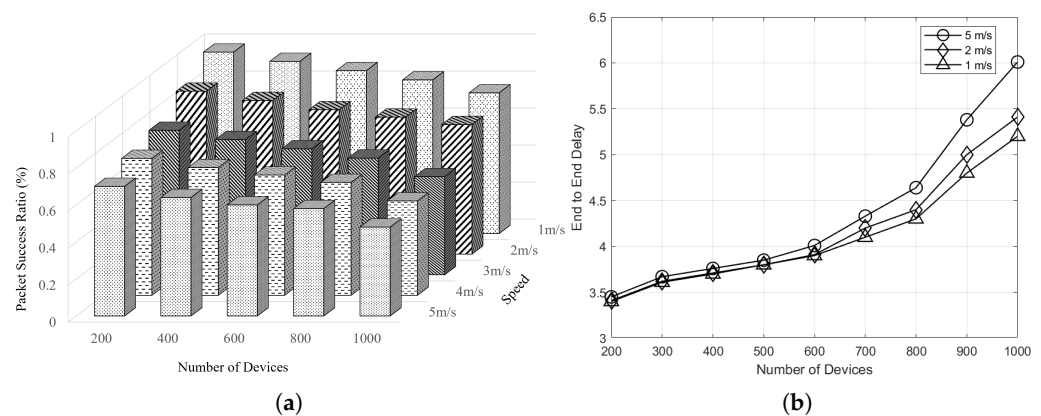

(a) (b)

Figure 4. Plots of the impact of speed and the number of devices. Analyzing the packet success ratio and end-to-end delay in the proposed AMILCC scheme: (**a**) Packet success ratio as a function of the number of devices and speed (m/s); (**b**) End-to-end delay as a function of the number of devices with varying speeds.

Figure 4b demonstrates the average end-to-end delay for packets reaching the GW in the AMILCC scheme, considering the number of devices and their respective mobility speeds within the network. The average delay remains consistent for LDs ranging from 200 to 600 at movement speeds of 1, 2, and 5 m/s. However, divergence emerges at varying speeds when the number of mobile LDs surpasses 600. This significant increase in delay is because of a combination of higher mobility speeds and a greater number of mobile devices, which induce frequent location changes, CH updates, and alterations in network resources. Consequently, this causes a considerable delay in the transmission of data to the GW.

Next, we compare the proposed AMILCC scheme to stationary schemes [17,19,20,30] namely the static cluster scheme, the FSRC scheme (also called the relay scheme), the mesh scheme, the cluster-based scheme, and the SFPCR scheme. These stationary schemes are utilized as baselines, where LDs remain static for the duration of the simulation, and the standard network-based ADR mechanism is used. In this analysis, the packet success ratio, energy consumption, and packet loss ratio are considered. This study validates the suggested technique for adaptive mobility-based IoT LoRa networks by using mobile clustering and adaptive resource allocation approaches in the corresponding SF regions.

Figure 5a demonstrates a relationship between the distance of LDs from the GW and their packet success ratio. The packet success ratio of all schemes diminishes exponentially with rising average distances. In particular, the proposed AMILCC scheme outperforms the stationary schemes as a result of the use of the HADR mechanism, which dynamically optimizes transmission parameters based on LQ and adaptively assigns SFs as optimal resources to LDs. This reduces retransmissions and significantly enhances the PSR. Additionally, the mobility of these LDs results in diverse signal paths and frequency variations, enabling multiple potential transmission routes and improved frequency diversity, which

helps overcome interference. Subsequently, at a distance between 3 km and 4 km, the SFPCR scheme and the FSRC scheme exhibit a modest enhancement in their packet success ratios, attributed to their utilization of relays to extend packets from distant LDs to the GW compared to the traditional static cluster and mesh schemes.
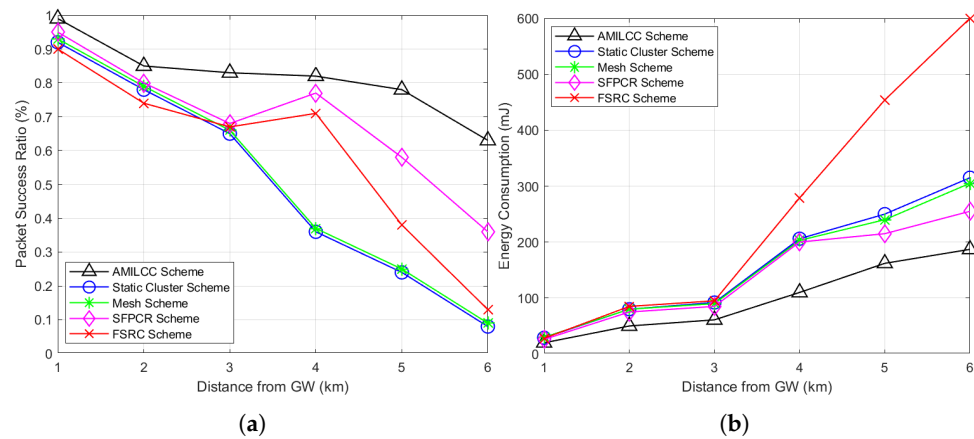

Figure 5. Plots of the performance evaluation metrics. The packet success ratio and energy consumption plotted against the distance from the GW with a 30-byte payload for various schemes: (**a**) Packet success ratio as a function of the distance from the GW (km); (**b**) Energy consumption as a function of the distance from the GW (km).

In Figure 5b, all schemes illustrate a relatively lower quantity of energy dissipation for LDs in close proximity to the GW. Nevertheless, beyond 3 km, the FSRC scheme consumes significantly more energy than the other stationary schemes because of broadcasts made by relays and source nodes. The percentage differences between the AMILCC scheme and the existing SFPCR, mesh, static cluster, and FSRC schemes are approximately 36.73%, 46.15%, 47.12%, and 90.21%, respectively. The results demonstrate that the proposed AMILCC scheme consumes the least amount of energy as the distance increases and the number of transmissions is regulated because all distant nodes in the high SF region propagate their transmission through the mobile CHs rather than direct transmission of packets to the GW, which minimizes the ToA. Overall, the energy consumption of the AMILCC is lower than that of the static schemes due to short-range communication for nodes to relay data to their CH and a higher packet success ratio since the scheme not only adaptively assigns an optimal SF before an uplink packet transmission but also has the capability to adapt to the variable channel and mobility conditions, thus leading to a small number of retransmissions that consume less power.

Figure 6 shows how the packet success ratio and energy consumption of LDs vary with the number of devices. In Figure 6a, all the schemes exhibit an inverse proportionality between the packet success ratio and the number of devices. An increase in the number of LDs culminates in a decreasing chance of packets successfully reaching the GW for the mesh, cluster-based, and FSRC schemes. This is due to the capture effect as nodes compete for the channel, leading to collisions arising from blind transmissions. These nodes transmit data packets as soon as they are ready to transmit, which hinders the successful delivery of packets to the GW. In contrast, the proposed AMILCC and SFPCR schemes employ collision-free transmission [50]. Due to this regulated access to the medium, each LD transmits its packets directly to either a CH, relay, or GW. Specifically, the AMILCC scheme adaptively allocates resources (SF and Tx) to mobile LDs based on signal quality and receiver sensitivity, resulting in an enhanced PSR with limited transmission errors. Consequently, the AMILCC scheme not only outperforms other schemes with few mobile LDs by achieving a PSR improvement of more than 90% but also maintains its superiority as the number of LDs increases to 1000, owing to its good adaptation of the SF. However, it has also been observed that as the number of LDs increases in the sensor area, it causes a

detrimental effect on the network's performance as a result of massive packet loss caused by significant congestion and vulnerability to interference.
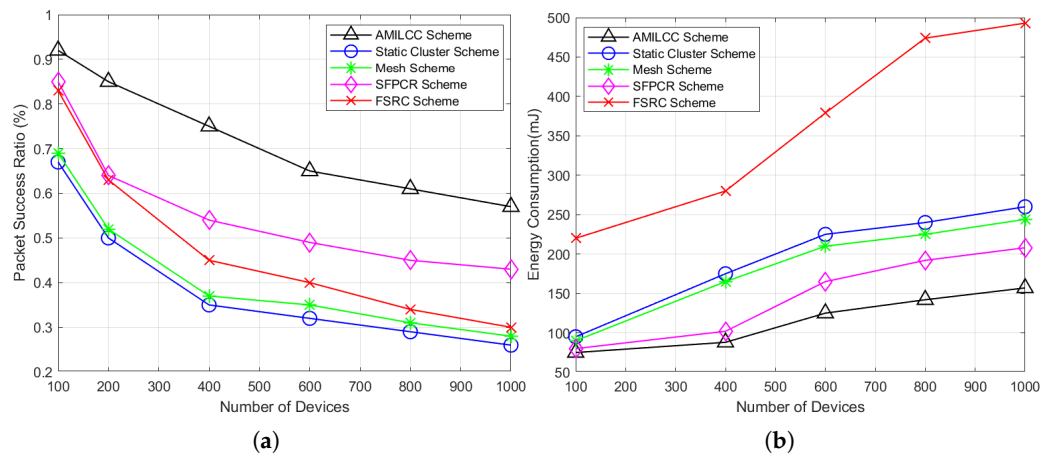

Figure 6. Plots of the performance evaluation metrics. The packet success ratio and energy consumption plotted against the number of devices of various schemes: (**a**) Packet success ratio as a function of the number of devices; (**b**) Energy consumption as a function of the number of devices.

Figure 6b depicts the variation in the number of devices as a function of the energy consumption for the proposed AMILCC scheme and the stationary schemes under consideration. In contrast to the AMILCC scheme, the results for all four comparative stationary schemes illustrate a direct increasing trend between energy consumption and the number of devices. In the FSRC scheme, the energy consumption rises quickly with the growing number of LDs exceeding 200 mJ as a result of using more LDs with a higher SF, making eight or more retransmission attempts with failure, and broadcasting packets sent throughout the network, which introduces considerable routing overhead and consumes more energy. Similar to the static cluster-based scheme, which has huge cluster sizes, the cluster member nodes must connect with other nodes located in the higher SF regions, resulting in increased energy consumption owing to intracluster distance communication and more attempts on the channels. Therefore, high energy consumption is observed, as the transmit energy consumption is primarily based on the values of the SF, Tx, and ToA. Overall, the energy consumption of the proposed AMILCC is lower than that of the stationary schemes as a result of the higher PSR and smaller number of retransmissions.

Figure 7a vividly shows an inverse proportionality between the packet success ratio and payload size (B) for the proposed AMILCC scheme and other comparative schemes. An increase in the payload size has a negative impact on network efficacy. Consequently, the smaller the size of a data payload, the higher the PSR. With a default payload size of 30 bytes, the PSRs of the AMILCC, SFPCR, FSRC, mesh, and static cluster schemes are approximately 80%, 64%, 45%, 40%, and 36%, respectively. The enhanced performance of the proposed AMILCC is primarily due to the deployed mobility model, clustering, and efficient adaptive data rate algorithms for optimizing the data rate and payload size. Therefore, the deteriorating PSR for all the schemes with an increase in the payload sizes may cause network congestion. As more nodes attempt to simultaneously transmit larger packets, collisions and contention for the communication medium may increase. This may result in increased packet loss and a lower PSR. Thus, to optimize the PSR in a mobile IoT LoRa environment, it is recommended that the payload size be as small as feasible.

Figure 7b depicts a direct proportionality between the energy consumption and payload sizes for all schemes. As the payload size increases, so does the energy consumption, limiting the lifespan of an IoT network that is energy-constrained. The energy consumption of the FSCR scheme rises quickly with the growing payload size due to the broadcast storm problem caused by source nodes and relay nodes deployed in the network and massive retransmission, which results in a bottleneck at the GW. Moreover, when a packet

is retransmitted multiple times with high SF and Tx, higher SFs are highly susceptible to interference due to the longer ToA over the wireless medium, which can negatively affect energy consumption. In comparison, the cluster-based, mesh, SFPCR, and proposed AMILCC schemes consume relatively little energy. Therefore, our results elucidate that the proposed scheme adaptively responds to mobility by allocating resources to the LDs to adjust the SF and Tx as soon as the location and environment change. Thus, optimizing LoRa parameters such as the SF, CR, and payload size is a key element in reducing the energy consumption of LDs. According to [51], increasing the payload size decreases the energy consumption per useful bit for high SF values. In contrast, for low SF values, payload size variations have a negligible impact on the energy per useful bit, although they do lead to increased ToA, a phenomenon also noted in our proposed AMILCC scheme.
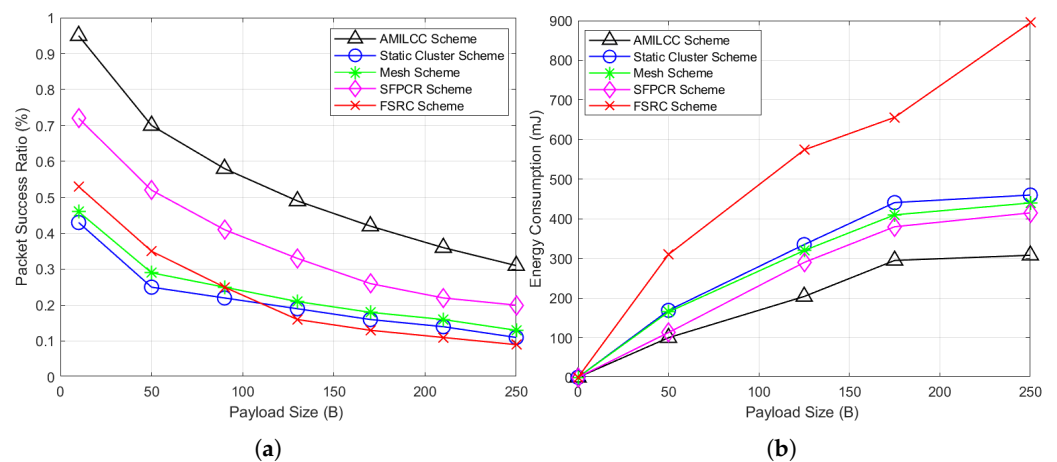

Figure 7. Plots of the performance evaluation metrics. The packet success ratio and energy consumption plotted against payloads of various schemes: (**a**) Packet success ratio as a function of the payload (B); (**b**) Energy consumption as a function of the payload (B).

6. Discussion

Our study highlights the impact of node mobility on the packet success ratio (PSR) and network performance within the AMILCC scheme, offering new insights compared to prior research [17,19–21,30]. Notably, node speeds up to 2 m/s allow the scheme to maintain a PSR above 70%, showcasing effective clustering of mobile LoRa devices compared to the results in [23,30], which exhibit their highest success probabilities of 50% and 65.7%, respectively. However, at speeds of 5 m/s, the PSR declines due to disruptions in stable connections, emphasizing the importance of managing mobility for optimal network performance. The AMILCC scheme's success in enhancing the PSR while reducing energy consumption through the hybrid adaptive data rate (HADR) mechanism marks a significant improvement over stationary schemes.

The AMILCC scheme has broad applicability in areas like asset tracking, industrial IoT, smart cities, smart metering, and agriculture, thanks to its optimization for mobile IoT LoRa networks. It promises improved mobile sensor reliability in urban monitoring, precise utility data collection in smart metering, and real-time agricultural management, facilitating better irrigation and pest control decisions. Its adaptability and energy efficiency position it as an ideal solution for elevating operational effectiveness and ensuring data accuracy across these sectors.

Trends in LoRa technology are gravitating toward more complex network architectures, such as multi-hop communication, to meet the demands for extended coverage and reliable data transmission in challenging environments. This shift is coupled with an increased focus on developing advanced network management protocols, aimed at enhancing energy and data efficiency in these sophisticated setups. This trend underscores the ongoing evolution and growing capabilities of LoRa technology in supporting diverse IoT applications.

7. Conclusions

In this paper, a novel adaptive mobility-based IoT LoRa clustering communication scheme was proposed to improve the connectivity, resource allocation, reliability, and packet success ratio in IoT LoRa networks. In the proposed AMILCC scheme, the network area was partitioned into several uneven regions to ensure optimal SF region allocation. We also provided an adaptive clustering method that generates clusters of mobile LDs within a given geographical distribution. We established a hybrid adaptive data rate mechanism to ideally allocate network resources to all mobile LDs to ensure efficient communication to the GW. We categorized this mechanism into intra-SF region HADR and inter-SF region HADR. Subsequently, we evaluated various speeds to ascertain the most suitable speed for the mobile LDs in the proposed AMILCC scheme. Specifically assessing the PSR, energy consumption, and end-to-end delay, we found that various mobility speeds (1, 2, and 5 m/s) influenced network performance. At movement speeds of 2 m/s or below, the proposed AMILCC scheme could easily cluster mobile LDs, achieving good performance in successfully delivering data packets to the GW.

Through comprehensive simulations, we demonstrated that our AMILCC scheme, harnessing low mobility speeds and utilizing the HADR mechanism, significantly optimized transmission parameters based on link quality and adaptively assigned SFs. This approach enhanced the packet success ratio to the GW by over 70% and reduced the end-to-end delay by 47.62%, indicating that our scheme outperformed the stationary schemes. Moreover, in terms of energy conservation, AMILCC surpassed other schemes, saving energy by an average of 55.05%. The mobility of these LDs resulted in diverse signal paths and frequency variations, enabling multiple potential transmission routes. In contrast, the stationary schemes utilized static LDs for the duration of the simulation and a standard network-based ADR mechanism. Moreover, the energy consumption of the proposed AMILCC was lower than that of the stationary schemes because of the higher PSR and the smaller number of retransmissions, which can prolong the lifetime of IoT LoRa networks in comparison to previous LoRa multi-hop schemes. Thus, the proposed scheme excels for mobile IoT applications, offering a high PSR and reliability with minimal energy consumption.

However, it is important to recognize certain limitations of the proposed AMILCC scheme. While it can significantly improve network performance and energy efficiency for mobile IoT LoRa applications, the dynamic nature of mobile LoRa devices and their energy consumption patterns may present challenges in balancing cluster head workloads and ensuring equitable energy usage across the network. Additionally, the scheme's reliance on specific mobility speeds and conditions might limit its applicability in environments with higher or more unpredictable mobility patterns. Addressing these limitations will be crucial for further enhancing the robustness and adaptability of the scheme for diverse IoT applications in future work.

Author Contributions: Conceptualization, D.M.; methodology, D.M.; software, Y.N.; validation, Y.N., H.C., and Y.S.; writing—original draft preparation, D.M.; writing—review and editing, Y.N. and E.L.; supervision, E.L. All authors have read and agreed to the published version of the manuscript.

Institutional Review Board Statement: Not applicable.

Informed Consent Statement: Not applicable.

Data Availability Statement: Available upon request.

Conflicts of Interest: The authors declare no conflicts of interest.

References

1. Ayoub, W.; Samhat, A.E.; Nouvel, F.; Mroue, M.; Prévotet, J.-C. Internet of mobile things: Overview of lorawan, dash7, and nb-iot in lpwans standards and supported mobility. *IEEE Commun. Surv. Tutor.* **2018**, *21*, 1561–1581. [CrossRef]
2. Chanal, P.M.; Kakkasageri, M.S. Security and privacy in IOT: A survey. *Wirel. Pers. Commun.* **2020**, *115*, 1667–1693. [CrossRef]
3. Bandyopadhyay, D.; Sen, J. Internet of things: Applications and challenges in technology and standardization. *Wirel. Pers. Commun.* **2011**, *58*, 49–69. [CrossRef]
4. Miorandi, D.; Sicari, S.; Pellegrini, F.D.; Chlamtac, I. Internet of things: Vision, applications and research challenges. *Ad Hoc Netw.* **2012**, *10*, 1497–1516. [CrossRef]
5. Zaman, S.; Khandaker, M.R.; Khan, R.T.; Tariq, F.; Wong, K.-K. Thinking Out of the Blocks: Holochain for Distributed Security in IoT Healthcare. *IEEE Access* **2022**, *10*, 37064– 37081. [CrossRef]
6. Zhang, W.-Z.; Elgendy, I.A.; Hammad, M.; Iliyasu, A.M.; Du, X.; Guizani, M.; El-Latif, A.A.A. Secure and optimized load balancing for multitier IoT and edge-cloud computing systems. *IEEE Internet Things J.* **2020**, *8*, 8119–8132. [CrossRef]
7. Yao, J.; Ansari, N. Enhancing federated learning in fogaided IoT by CPU frequency and wireless power control. *IEEE Internet Things J.* **2020**, *8*, 3438–3445. [CrossRef]
8. Perera, C.; Liu, C.H.; Jayawardena, S. The emerging internet of things marketplace from an industrial perspective: A survey. *IEEE Trans. Emerg. Top. Comput.* **2015**, *3*, 585–598. [CrossRef]
9. Anagnostopoulos, T.; Zaslavsky, A.; Kolomvatsos, K.; Medvedev, A.; Amirian, P.; Morley, J.; Hadjieftymiades, S. Challenges and opportunities of waste management in IoT-enabled smart cities: A survey. *IEEE Trans. Sustain. Comput.* **2017**, *2*, 275–289. [CrossRef]
10. Shafique, K.; Khawaja, B.A.; Sabir, F.; Qazi, S.; Mustaqim, M. Internet of things (IoT) for next-generation smart systems: A review of current challenges, future trends and prospects for emerging 5G-IoT scenarios. *IEEE Access* **2020**, *8*, 23022– 23040. [CrossRef]
11. Raghuvanshi, A.; Singh, U.K.; Joshi, C. A review of various security and privacy innovations for IoT applications in healthcare. In *Advanced Healthcare Systems: Empowering Physicians with IoT-Enabled Technologies*; Scrivener Publishing LLC: Beverly, MA, USA, 2022; pp. 43–58. [CrossRef]
12. Nahrstedt, K.; Li, H.; Nguyen, P.; Chang, S.; Vu, L. Internet of mobile things: Mobility-driven challenges, designs and implementations. In Proceedings of the 2016 IEEE First International Conference on Internet-of-Things Design and Implementation (IoTDI), Berlin, Germany, 4–8 April 2016; pp. 25–36. [CrossRef]
13. Council, N.; Nic, N.; Intelligence, S. Disruptive Civil Technologies: Six Technologies with Potential Impacts on Us Interests out to 2025. Conference Report CR. 2008. Volume 2007. Available online: https://irp.fas.org/nic/disruptive.pdf (accessed on 21 November 2023).
14. Available online: https://www.ericsson.com/4ae28d/assets/local/reports-papers/mobility-report/documents/2022/ericsson-mobility-report-november-2022.pdf (accessed on 30 November 2023).
15. Sornin, N.; Luis, M.; Eirich, T.; Kramp, T.; Hersent, O. *Lorawan Specification*; LoRa Alliance: Fremont, CA, USA, 2015; Volume 1.
16. Lavric, A.; Petrariu, A.I.; Popa, V. SigFox communication protocol: The new era of IoT? In Proceedings of the 2019 International Conference on Sensing and Instrumentation in IoT Era (ISSI), Lisbon, Portugal, 29–30 August 2019; pp. 1–4.
17. Lee, S.; Lee, J.; Park, H.-S.; Choi, J.K. A novel fair and scalable relay control scheme for Internet of Things in LoRabased low-power wide-area networks. *IEEE Internet Things J.* **2020**, *8*, 5985–6001. [CrossRef]
18. Lyu, J.; Yu, D.; Fu, L. Achieving max-min throughput in LoRa networks. In Proceedings of the 2020 International Conference on Computing, Networking and Communications (ICNC), Big Island, HI, USA, 17–20 February 2020; pp. 471–476. [CrossRef]
19. Zhu, G.; Liao, C.H.; Sakdejayont, T.; Lai, I.W.; Narusue, Y.; Morikawa, H. Improving the capacity of a mesh LoRa network by spreading-factor-based network clustering. *IEEE Access* **2019**, *7*, 21584–21596. [CrossRef]
20. Lee, H.-C.; Ke, K.-H. Monitoring of large-area IoT sensors using a LoRa wireless mesh network system: Design and evaluation. *IEEE Trans. Instrum. Meas.* **2018**, *67*, 2177–2187. [CrossRef]
21. Al Mojamed, M. On the Use of LoRaWAN for Mobile Internet of Things: The Impact of Mobility. *Appl. Syst. Innov.* **2021**, *5*, 5. [CrossRef]
22. Benkahla, N.; Tounsi, H.; Ye-Qiong, S.; Frikha, M. Enhanced ADR for LoRaWAN networks with mobility. In Proceedings of the 2019 15th International Wireless Communications & Mobile Computing Conference (IWCMC), Tangier, Morocco, 24–28 June 2019; pp. 1–6. [CrossRef]
23. Farhad, A.; Pyun, J.-Y. HADR: A Hybrid Adaptive Data Rate in LoRaWAN for Internet of Things. *ICT Express* **2022**, *8*, 283–289. [CrossRef]
24. Finnegan, J.; Brown, S.; Farrell, R. Evaluating the scalability of LoRaWAN gateways for class B communication in ns-3. In Proceedings of the 2018 IEEE Conference on Standards for Communications and Networking (CSCN), Paris, France, 29–31 October 2018; pp. 1–6. [CrossRef]
25. Sisinni, E.; Ferrari, P.; Carvalho, D.F.; Rinaldi, S.; Marco, P.; Flammini, A.; Depari, A. LoRaWAN range extender for Industrial IoT. *IEEE Trans. Ind. Inform.* **2019**, *16*, 5607–5616. [CrossRef]
26. Zorbas, D.; Papadopoulos, G.Z.; Maille, P.; Montavont, N.; Douligeris, C. Improving LoRa network capacity using multiple spreading factor configurations. In Proceedings of the 2018 25th International Conference on Telecommunications (ICT), Saint-Malo, France, 26–28 June 2018; pp. 516–520. [CrossRef]
27. Bor, M.C.; Vidler, J.; Roedig, U. LoRa for the Internet of Things. *Ewsn* **2016**, *16*, 361–366.

28. Mugerwa, D.; Nam, Y.; Cho, H.; Choi, H.; Shin, Y.; Lee, E. Implicit Multi-hop Communication Scheme based on Overhearing in IoT LoRa Networks. In Proceedings of the 2022 Thirteenth International Conference on Ubiquitous and Future Networks (ICUFN), Barcelona, Spain, 5–8 July 2022; pp. 190–195. [CrossRef]
29. Mai, D.L.; Kim, M.K. Multi-Hop LoRa network protocol with minimized latency. *Energies* **2020**, *13*, 1368. [CrossRef]
30. Mugerwa, D.; Nam, Y.; Choi, H.; Shin, Y.; Lee, E. SF-Partition-Based Clustering and Relaying Scheme for Resolving Near–Far Unfairness in IoT Multihop LoRa Networks. *Sensors* **2022**, *22*, 9332. [CrossRef] [PubMed]
31. Temene, N.; Sergiou, C.; Georgiou, C.; Vassiliou, V. A survey on mobility in Wireless Sensor Networks. *Ad Hoc Netw.* **2022**, *125*, 102726. [CrossRef]
32. Torres, N.; Martins, P.; Pinto, P.; Lopes, S.I. Smart & Sustainable Mobility on Campus: A secure IoT tracking system for the BIRA Bicycle. In Proceedings of the 2021 16th Iberian Conference on Information Systems and Technologies (CISTI), Chaves, Portugal, 23–26 June 2021; pp. 1–7. [CrossRef]
33. Robbe, B.; Danny, W. A qos-aware adaptive mobility handling approach for lora-based iot systems. In Proceedings of the 2018 IEEE 12th International Conference on Self-Adaptive and Self-Organizing Systems (SASO), Trento, Italy, 3–7 September 2018; pp. 130–139. [CrossRef]
34. Kim, S.; Koack, M.; Choo, S.; Kim, S. Analysing Spatial Usage Characteristics of Shared E-scooter: Focused on Spatial Autocorrelation Modeling. *J. Korea Inst. Intell. Transp. Syst.* **2021**, *20*, 54–69. [CrossRef]
35. Stankovic, J.A. Research directions for the internet of things. *IEEE Internet Things J.* **2014**, *1*, 3–9. [CrossRef]
36. Ayele, E.D.; Meratnia, N.; Havinga, P.J. Towards a new opportunistic IoT network architecture for wildlife monitoring system. In Proceedings of the 2018 9th IFIP International Conference on New Technologies, Mobility and Security (NTMS), Paris, France, 26–28 February 2018; pp. 1–5. [CrossRef]
37. Sciullo, L.; Trotta, A.; Di Felice, M. Design and performance evaluation of a LoRa-based mobile emergency management system (LOCATE). *Ad Hoc Netw.* **2020**, *96*, 101993. [CrossRef]
38. Martinez-Caro, J.-M.; Cano, M.-D. IoT system integrating unmanned aerial vehicles and LoRa technology: A performance evaluation study. *Wirel. Commun. Mob. Comput.* **2019**, *2019*, 4307925. [CrossRef]
39. Andrei, M.L.; Rădoi, L.A.; Tudose, D.Ş. Measurement of node mobility for the LoRa protocol. In Proceedings of the 2017 16th RoEduNet Conference: Networking in Education and Research (RoEduNet), Targu Mures, Romania, 21–23 September 2017; pp. 1–6. [CrossRef]
40. Mohammadi, S.; Farahani, G. Scalability Analysis of a LoRa Network Under Inter-SF and Co-SF Interference with Poisson Point Process Model. *J. Comput. Secur.* **2021**, *8*, 43–57. [CrossRef]
41. Magrin, D.; Centenaro, M.; Vangelista, L. Performance evaluation of LoRa networks in a smart city scenario. In Proceedings of the 2017 IEEE International Conference on communications (ICC), Paris, France, 21–25 May 2017; pp. 1–7. [CrossRef]
42. Philip, M.S.; Singh, P. Energy consumption evaluation of LoRa sensor nodes in wireless sensor network. In Proceedings of the 2021 Advanced Communication Technologies and Signal Processing (ACTS), Virtual, 15–17 December 2021; pp. 1–4. [CrossRef]
43. Lee, S.-G.; Lee, H.-J. Performance of Mobility Models for Routing Protocol in Wireless Ad-hoc Networks. *J. Inf. Commun. Converg. Eng.* **2011**, *9*, 610–614.
44. Sharma, S.; Kumar, S. Estimation of Mobility Models Based on Mobility Metrics and Their Impact on Routing Protocols in MANET. *Int. J. Comput. Commun. Eng.* **2013**, *2*, 386. [CrossRef]
45. Wang, X.; Mu, Y. Research on Grey Relational Clustering Model of Multiobjective Human Resources Based on Time Constraint. *Sci. Program.* **2021**, *2021*, 5551255.. [CrossRef]
46. Khan, M.M.R.; Siddique, M.A.B.; Arif, R.B.; Oishe, M.R. ADBSCAN: Adaptive density-based spatial clustering of applications with noise for identifying clusters with varying densities. In Proceedings of the 2018 4th International Conference on Electrical Engineering and Information & Communication Technology (iCEEiCT), Dhaka, Bangladesh, 13–15 September 2018; pp. 107–111. [CrossRef]
47. Carlsson, A.; Kuzminykh, I.; Franksson, R.; Liljegren, A. Measuring a LoRa network: Performance, possibilities and limitations. In Proceedings of the Internet of Things, Smart Spaces, and Next Generation Networks and Systems: 18th International Conference, NEW2AN 2018, and 11th Conference, ruSMART 2018, St. Petersburg, Russia, 27–29 August 2018; Proceedings 18; pp. 116–128. [CrossRef]
48. Farhad, A.; Kim, D.-H.; Kim, B.-H.; Mohammed, A.F.Y.; Pyun, J.-Y. Mobility-aware resource assignment to IoT applications in long-range wide area networks. *IEEE Access* **2020**, *8*, 186111–186124. [CrossRef]
49. Al-Qadami, N.; Laila, I.; Koucheryavy, A.; Ahmad, A.S. Mobility adaptive clustering algorithm for wireless sensor networks with mobile nodes. In Proceedings of the 2015 17th International Conference on Advanced Communication Technology (ICACT), PyeongChang, Republic of Korea, 1–3 July 2015; pp. 121–126. [CrossRef]
50. Zorbas, D.; O'Flynn, B. Autonomous collision-free scheduling for LoRa-based industrial Internet of Things. In Proceedings of the 2019 IEEE 20th International Symposium on A World of Wireless, Mobile and Multimedia Networks(WoWMoM), Washington, DC, USA, 10–12 June 2019; pp. 1–5. [CrossRef]
51. Maudet, S.; Andrieux, G.; Chevillon, R.; Diouris, J.-F. Refined node energy consumption modeling in a LoRaWAN network. *Sensors* **2021**, *21*, 6398. [CrossRef] [PubMed]